

The Binding Site of Acetylcholine Receptor as Visualized in the X-Ray Structure of a Complex between α -Bungarotoxin and a Mimotope Peptide

Michal Harel,^{1,8} Roni Kasher,^{2,8} Anne Nicolas,¹ J. Mitchell Guss,^{1,9} Moshe Balass,² Mati Fridkin,³ August B. Smit,⁵ Katjuša Brejc,⁶ Titia K. Sixma,⁶ Ephraim Katchalski-Katzir,² Joel L. Sussman,¹ and Sara Fuchs^{4,7}

¹Department of Structural Biology

²Department of Biological Chemistry

³Department of Organic Chemistry

⁴Department of Immunology
Weizmann Institute of Science
Rehovot 76100
Israel

⁵Department of Molecular and Cellular
Neurobiology

Vrije Universiteit
De Boelelaan 1087
1081 HV Amsterdam
The Netherlands

⁶Division of Molecular Carcinogenesis
Netherlands Cancer Institute
Plesmanlaan 121
1066 CX Amsterdam
The Netherlands

Summary

We have determined the crystal structure at 1.8 Å resolution of a complex of α -bungarotoxin with a high affinity 13-residue peptide that is homologous to the binding region of the α subunit of acetylcholine receptor. The peptide fits snugly to the toxin and adopts a β hairpin conformation. The structures of the bound peptide and the homologous loop of acetylcholine binding protein, a soluble analog of the extracellular domain of acetylcholine receptor, are remarkably similar. Their superposition indicates that the toxin wraps around the receptor binding site loop, and in addition, binds tightly at the interface of two of the receptor subunits where it inserts a finger into the ligand binding site, thus blocking access to the acetylcholine binding site and explaining its strong antagonistic activity.

Introduction

The nicotinic acetylcholine receptor (AChR) is a ligand-gated ion channel activated by binding of acetylcholine (ACh) (for reviews see Changeux and Edelstein, 1998; Karlin and Akabas, 1995). α -Neurotoxins, such as α -bungarotoxin (α -BTX), behave as competitive antagonists of ACh for its site (Changeux et al., 1970; Lee and Chang, 1966). They bind specifically and with high affinity to

AChR and exhibit high toxicity due to inhibition of AChR function at the neuromuscular junction. Synthetic peptides that bind to α -BTX may serve as competitive inhibitors of α -BTX binding to AChR, and hence provide potential lead compounds for antidotes against α -BTX poisoning.

The X-ray structure of AChR has not yet been solved since its hydrophobic character hampers its successful crystallization. There have been several attempts to crystallize the extracellular domain of AChR α subunit and most recently, the X-ray structure of an acetylcholine binding protein (AChBP), a water-soluble homolog of the nicotinic AChR ligand binding domain isolated from snail, has been solved (Brejc et al., 2001). The high affinity and specific interaction of α -BTX with AChR has been of considerable importance in the study of the ligand binding site of AChR. The ligand binding site of AChR is located mainly at the α subunit, in the vicinity of Cys192 and Cys193 (Kao et al., 1984; Neumann et al., 1985), though residues in the interface of neighboring subunits contribute also to the binding site (Changeux and Edelstein, 1998; Karlin and Akabas, 1995 and references cited therein). Short synthetic peptides derived from this region of the AChR α subunit were shown to bind α -BTX (Lentz, 1995; Neumann et al., 1986a). A 12-mer synthetic peptide corresponding to residues 185–196 of the AChR, and encompassing the two tandem cysteines, was found to bind agonists specifically and to inhibit the binding of α -BTX to AChR with an IC_{50} of 10^{-4} M (Neumann et al., 1986a, 1986b).

Additional information on the α -BTX binding site in the AChR molecule came from our previous study employing a random combinatorial phage-display peptide library (Balass et al., 1997). We have identified a library lead peptide (MRYYESLKSYPD) that binds α -BTX and inhibits its binding to AChR with an IC_{50} in the low-micromolar range. This peptide contains the motif YYXSS that is homologous to the AChR consensus motif YYXCC₁₉₃, located at the ligand binding site. Alignment of the library lead peptide with the corresponding amino acid residues in AChR resulted in a 13-mer peptide corresponding to residues 187–199 of the *Torpedo californica* AChR (TcAChR) α subunit, which inhibits the binding of α -BTX to AChR with an IC_{50} of 10^{-6} M (Balass et al., 1997). The structure of the complex between α -BTX and the library lead peptide has been determined using 2D ¹H-NMR (Scherf et al., 1997). The amino acid residues in the library lead peptide that interact with α -BTX were identified and it was shown that the bound peptide adopts a loop conformation around a hydrophobic core created by a side chain of Tyr197 of the peptide (peptide numbering follows the α subunit numbering—see Table 1).

In a recent study (Kasher et al., 2001), we employed NMR-derived structural information of the complex of α -BTX with the lead peptide (Scherf et al., 1997), along with other structural and functional features of the AChR system (Barchan et al., 1995; Kachalsky et al., 1995; Neumann et al., 1989), to design and prepare peptides that interact with α -BTX with increased affinity. We used

⁷ Correspondence: sara.fuchs@weizmann.ac.il

⁸ These authors contributed equally to this work.

⁹ Permanent address: Department of Biochemistry, University of Sydney, N.S.W. 2006, Australia.

Table 1. Sequence of HAP and Related Peptides and Their Inhibition of α -BTX Binding to AChR

Peptide	187	188	189	190	191	192	193	194	195	196	197	198	199	200	IC ₅₀ (M) ^a
Lead peptide	M	R	Y	Y	E	S	S	L	K	S	Y	P	D		3.3×10^{-7}
HAP	<u>W</u>	<u>R</u>	<u>Y</u>	<u>Y</u>	<u>E</u>	S	S	L	L	<u>P</u>	<u>Y</u>	<u>P</u>	<u>D</u>		1.9×10^{-9}
HAP#2	W	R	Y	Y	E	S	S	L	E	P	Y	P	D		2.0×10^{-9}
HAP#3	W	R	Y	Y	E	S	S	L	D	P	Y	P	D		3.8×10^{-9}
HAP#4	W	R	Y	Y	E	C	C	L	D	P	Y	P	D		1.9×10^{-9}
HAP#5	W	R	Y	Y	E	S	S	L	K	P	Y	P	D		1.0×10^{-8}
Muscle TcAChR 187–200 (α 1)	W	V	Y	Y	T	C	C	P	D	T	P	Y	L	D	2.6×10^{-8}
Neuronal rat brain AChR 187–199 (α 7)	E	K	F	Y	E	C	C	K	E	P	Y	P	D		1.8×10^{-5}
AChBP 182–194 ^b	S	V	T	Y	S	C	C	P	E	A	Y	E	D		ND ^c

Identical residues in the HAP and either TcAChR α 1 or rat brain α 7 subunits (both of which bind α -BTX) are in italics and underlined.

Residues in bold are HAP residues different from the lead peptide.

^aData are from Kasher et al. (2001).

^bAChBP sequence from Smit et al. (2001).

^cNot determined.

the phage-library peptide MRYYESSLLKSYDP (Balass et al., 1997) as the lead peptide, and designed a new restricted combinatorial peptide library based on rational replacement of a limited number of amino acid residues in the lead peptide. Several peptides that bind α -BTX with high affinity and inhibit its binding to TcAChR with an IC₅₀ in the *nanomolar* range have been produced (Table 1). This affinity is in the range of that reported for the binding of α -BTX to the AChR α subunit (Tzartos and Changeux, 1984). The inhibitory potency of the high affinity peptides (HAP) is at least two orders of magnitude better than the inhibition obtained by the original phage library lead peptide (Balass et al., 1997), and one order of magnitude or more better than any synthetic peptide (13–17 residues long) corresponding to sequences from the α -BTX binding site of AChR (Table 1).

In the present study, we have determined the crystal structure of the complex formed between one HAP (WRYYESSLLKSYDP) and α -BTX at 1.8 Å resolution. This HAP differs from the library lead peptide by only three residues; however, this difference causes an increase in its binding to α -BTX, by more than two orders of magnitude. We have demonstrated that this HAP fits snugly to the toxin, making numerous interactions with three of its fingers. It assumes a loop conformation, with two β strand sections, one of which makes a β sheet with an α -BTX strand. The structural data can be used for the design of peptide ligands having a desired highly specific biological activity and contribute to resolving the fine structure of the AChR ligand binding site in general. The structure of the peptide and the homologous loop of the AChBP, a soluble analog of the extracellular domain of the acetylcholine receptor, are remarkably similar. From this it was possible to construct a detailed model of the interaction of α -BTX with the pentameric AChBP, and by analogy, to see the interaction of α -BTX with the AChR. The toxin is seen to wrap around the receptor binding site loop, and in addition, to bind tightly, in an interlocking fashion, at the interface of two of the receptor subunits where it inserts a finger into the ligand binding site. This reveals how the toxin blocks access to the acetylcholine binding site and thus explains its strong antagonistic activity.

Results and Discussion

The Crystal Structure of α -BTX-HAP

A co-crystal of α -BTX with the high affinity peptide WRYYESSLLKSYDP was grown, and designated α -BTX-HAP. This is a novel report on a crystal structure of a complex of α -BTX with an AChR-related peptide. The refined structure of α -BTX-HAP contains two monomers of α -BTX and two associated 13-mer peptides in the asymmetric unit. The final R factor is 20.2%, and R free is 23.5%. The quality parameters of the refined structure are listed in Table 2. The Ramachandran plot for the structure shows no residues in disallowed regions (Figure 1). The structure contains 217 water molecules. The crystallographic packing produces two kinds of 2-fold related dimers. The crystallographic dimer of monomers A–A displays a continuous β sheet area across the 2-fold axis perpendicular to the β strands, similar to the one seen in the X-ray structure of α -BTX (Protein Data Bank ID code 2abx) (Love and Stroud, 1986), even though the unit cell and space group are different. In this dimer, the two HAP peptides are situated far apart (ca. 40 Å) from each other (Figure 2a). The crystallographic dimer of monomers B–B has a 2-fold axis in the plane of the β strands (Figure 2b). The two monomers, with their associated HAPs, were refined independently. The RMS deviation of the C α 's of the α -BTX monomers A and B is 0.64 Å (using all 74 residues) and of the HAPs associated with monomers A and B (using 12 residues of the HAP) is 0.68 Å (Table 3). Differences larger than 1.2 Å are seen in three loops of the two independent α -BTX molecules. The two HAPs show a large C α difference (1.5 Å) only in their N-terminal Trp position. The monomers show surprising differences in their average temperature factors, 22.2 Å⁻² for α -BTX monomer A, and 27.7 Å⁻² for monomer B. Monomer A also displays significantly more residues with alternate conformation (see below), and all 13 residues in its associated HAP can be seen, but only 12 in monomer B complex. The higher degree of order in monomer A may be due to its crystal packing environment. Monomer A, together with its associated HAP, has 96 packing contacts (shorter than 3.6 Å) to symmetry-related molecules, while monomer B has only 50 such contacts. Dynamic light scattering

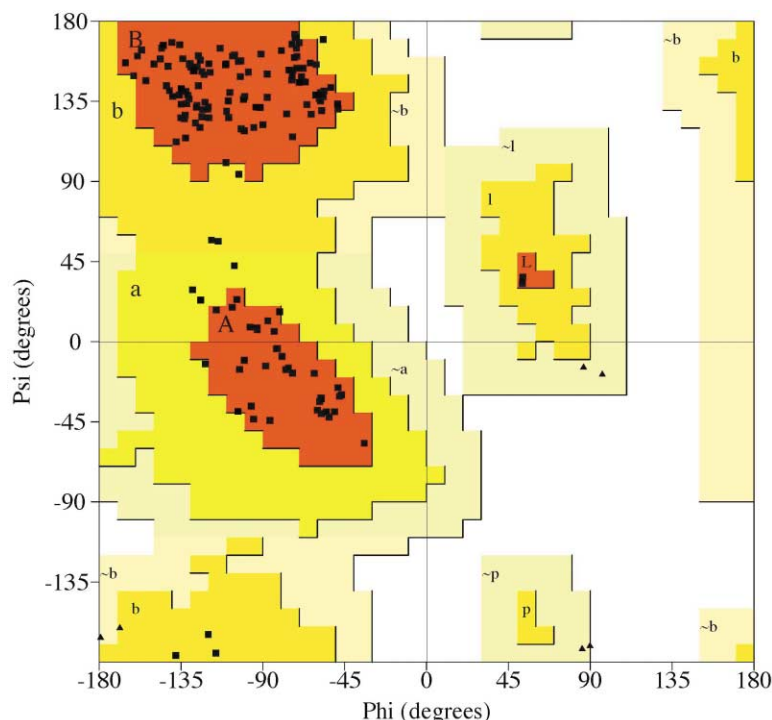


Figure 1. Ramachandran Plot for α -BTX-HAP
The plot was produced by PROCHECK
(Laskowski et al., 1993).

measurements on a complex between α -BTX and a peptide corresponding to residues 182–202 of *Torpedo* AChR α subunit have shown it to be monomeric at pH < 5.0 and dimeric at higher pH values (Samson et al., 2001). Since the crystal was grown at pH 7.5, it is possible that dimer of monomer A (Figure 2a), which is similar to the α -BTX dimer seen in the published structure (Protein Data Bank ID code 2abx), is present in solution.

Interactions of the HAP with α -BTX

The 13-mer HAP assumes an antiparallel β hairpin structure, and is held snugly between fingers 1, 2, and 4 of α -BTX (see Figures 2 and 3). Out of a total of 1,552 Å² of accessible surface area of HAP A, ca. 45% (682 Å²) becomes inaccessible upon its binding to α -BTX (Figure 3). The shortest and most numerous interactions are formed with finger 2 of α -BTX. The two arms of the HAP hairpin assume a β sheet conformation, with residues Arg188-Tyr190 making an intermolecular interaction with α -BTX residues Val39-Glu41, and residues Leu195-Tyr197 making an intramolecular interaction with Arg188-Tyr190. The short intramolecular interactions in the two copies of the HAP are listed in Table 4. Similar interactions have been recently demonstrated in an NMR study of the structure of a complex of α -BTX with another high affinity peptide (HAP#2 in Table 1) (Scherf et al., 2001). Moreover, the NMR structure of a complex of α -BTX with a library lead peptide differing by only three residues from the one studied here (Scherf et al., 1997) (Table 1) also shows a similar fold to the HAP and a similar binding site to α -BTX. However, in this case, the X-ray and NMR structures show some deviation (Table 3) mainly in the loop regions and the C termini. An NMR study (Samson et al., 2001) of the structure of the complex of α -BTX and a peptide corresponding to residues 182–202 of *TcAChR* showed that peptide to have also a β hairpin conformation with 2 short β sheet segments. However, that NMR structure shows a longer turn region with residues His186-Val188 and Tyr198-Asp200 of the peptide having the β sheet conformation, and the intermolecular interaction is with α -BTX residues Lys38-Val40. Surprisingly, a recent study on the NMR solution structure of a complex of α -BTX and a

Table 2. Crystallographic Data for α -BTX-HAP Complex

	α -BTX-HAP	α -BTX-HAP KI Soak
Unit cell (Å)	42.0, 153.4, 73.0	41.9, 151.5, 72.8
Resolution range (Å)	40–2.4	23.5–1.8
Number of unique reflections	9,611	22,265
Completeness (%)	99.5 (95.9) ^a	99.0 (99.1) ^a
R _{sym} (on I) (%)	11.6 (43.9) ^a	8.1 (59.4) ^a
I/ σ (I)	12.7 (2.6) ^a	14.0 (2.3) ^a
Number of protein atoms		1,334
Number of solvent atoms		217
Number of iodine atoms		2
R _{fact} (R _{free}) F > 0 σ		20.2% (23.5%)
RMS from ideality ^b		
Bond length (Å)		0.005
Bond angle (°)		1.5
Ramachandran plot ^c		
Favored		92.1%
Allowed		7.9%
Generously allowed		0.0%
Disallowed		0.0%

^a Statistics for outer shell 1.86–1.80 Å data in parentheses.

^b Calculated by module xtal_pdbsubmission of program CNS (Brünger et al., 1998).

^c Calculated by program PROCHECK (Laskowski et al., 1993).

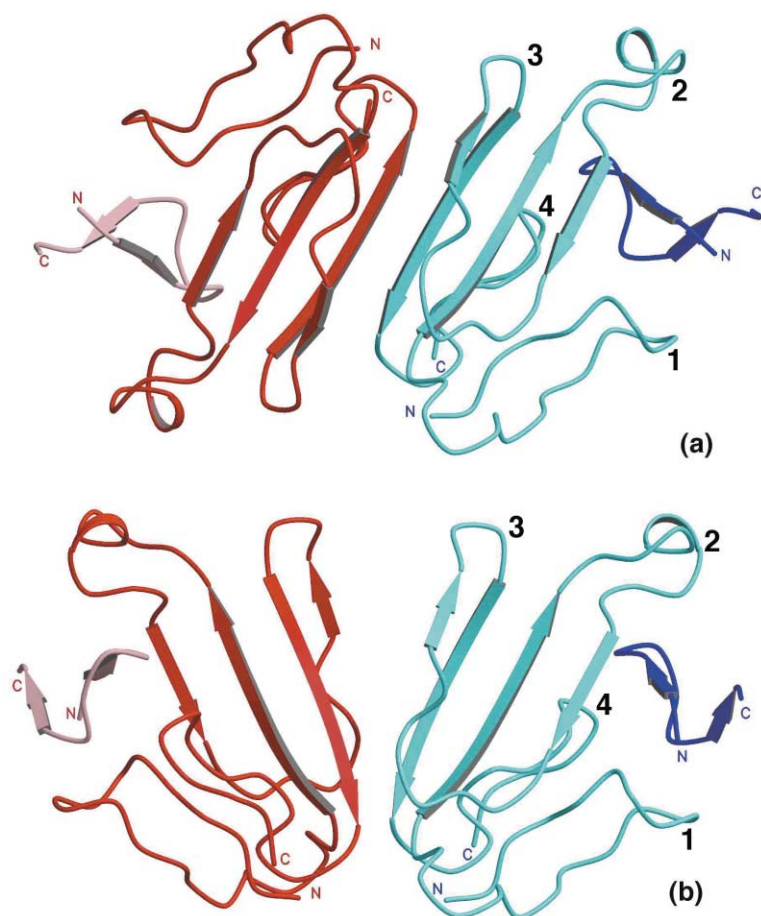


Figure 2. The Crystallographic Packing of the α -BTX-HAP in the Crystal Produces Two Kinds of Dimers

(a) Monomer A makes a 2-fold related dimer with a continuous β sheet area across the 2-fold axis which is perpendicular to the plane of the β strands, like the one seen in the α -BTX X-ray structure (Protein Data Bank ID code 2abx) with the two HAPs situated far apart (ca. 40 Å) from each other. (b) Dimer produced by monomer B by a 2-fold axis which lies in the plane of the β strands. The two HAPs are likewise far apart.

peptide corresponding to residues 181–198 of muscle type AChR did not demonstrate a β hairpin structure (Zeng et al., 2001). This could be due to the fact that only 11 intermolecular interactions were observed in that study. A previous NMR study of α -BTX complex with a dodecapeptide corresponding to residues 185–196 of the TcAChR α subunit (Basus et al., 1993) revealed that the bound peptide adopts an extended conformation, and interactions with α -BTX were formed only between a peptide segment corresponding to residues 186–190 of the receptor. Affinity labeling experiments which identified positions 10 and 33 of α -neurotoxin to be within 11.5–15.5 Å from AChR residues Cys192–Cys193 (Michalet et al., 2000) agree with the α -BTX-HAP structure where the corresponding C α distances are 11.05 Å

(Pro10–Ser193), 12.72 Å (Cys33–Ser193), 14.45 Å (Pro10–Ser192), 9.76 Å (Cys33–Ser192), respectively.

The HAP was found to inhibit α -BTX binding to TcAChR with IC₅₀ of 1.9×10^{-9} M while a peptide corresponding to the sequence 187–200 of TcAChR inhibited the binding with IC₅₀ of 2.6×10^{-8} M (Kasher et al., 2001), i.e., one order of magnitude weaker. This may be explained by the gain of four H bonds in the tightly binding N terminus of the HAP, i.e., in residues Arg188, Glu191, and Ser192 (Table 5), which are Val, Thr, and Cys in the TcAChR sequence.

As demonstrated in Figure 4, Tyr189 of the HAP forms a snug fit into a loop region of α -BTX. The formation of two H bonds from its hydroxyl to residues Thr8 and Ile11 of α -BTX (Table 5) makes the tyrosine at that position

Table 3. RMS Deviation of C α Positions in Å

	Monomer A	Number residues used
Monomer B	0.64	74
NMR α -BTX structure (PDB ID code 2btx)	4.03	74
Monomer A of α -BTX (PDB ID code 2 abx)	4.03	74
Neurotoxin-I (PDB ID code 1 ntn)	0.76	63
	HAP A	
HAP B	0.68	12
NMR lead peptide (PDB ID code 2btx)	2.15	13
ACh binding loop 182–193 of AChBP	0.76	12

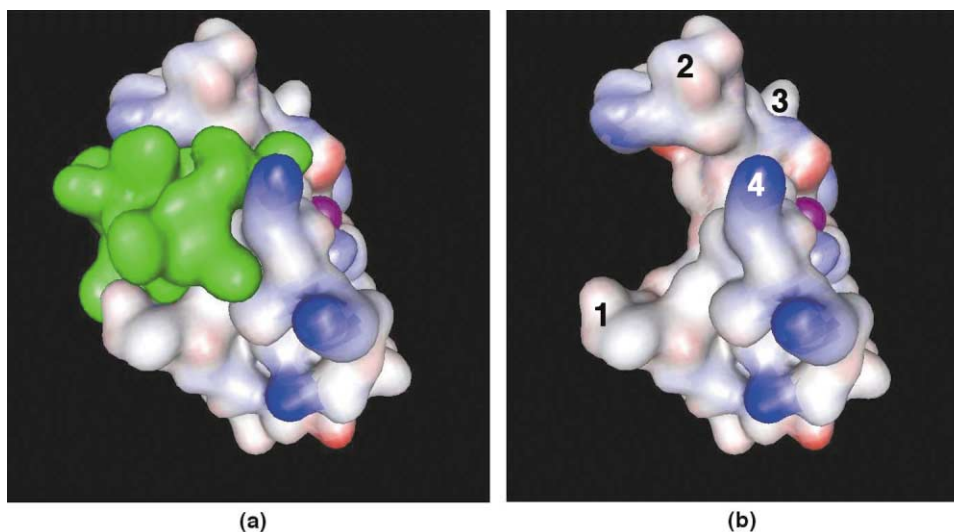


Figure 3. 3D Surface Drawing of the Structure of α -BTX-HAP

Color of the α -BTX corresponds to electrostatic charge, with blue positive and red negative (rendered with WebLabViewerLite software (MSI, 1998).

(a) α -BTX-HAP monomer A complex. HAP is shown in green.

(b) α -BTX monomer A with HAP removed.

an ideal candidate for forming binding interactions with α -BTX. Indeed, this tyrosine is known to play a crucial role in α -BTX binding. Muscle ($\alpha 1$) or neuronal ($\alpha 7$) AChRs that bind α -BTX all have a Tyr, or sometimes Phe, at position 189. It should be noted that there are no significant differences in the binding properties of AChRs containing Tyr or Phe at position 189. However, replacement of Tyr189 with Phe in the library lead peptide resulted in lowering the binding potency by one order of magnitude (Kasher et al., 2001). Muscle AChRs from animal species that are resistant to α -BTX (e.g. snake and mongoose) or neuronal AChRs that do not bind α -BTX have a nonaromatic residue at this position (Barchan et al., 1995). Neuronal AChR subunits $\alpha 2$, $\alpha 3$, and $\alpha 4$ have Lys at this position. The receptor complexes containing these subunits do not bind α -BTX. In contrast, the neuronal receptor containing $\alpha 7$, which has a Tyr at this position, does bind α -BTX. The X-ray structure shows that Tyr189 cannot be changed to Lys without clashes in the α -BTX binding cavity. This explains the resistance of neuronal $\alpha 2$, $\alpha 3$, and $\alpha 4$ AChRs to α -BTX. This is also supported by our previous findings demonstrating that the mutation Tyr189Lys in the lead peptide

or in the corresponding $\alpha 1$ and $\alpha 7$ peptides prohibits them from binding α -BTX (Balass et al., 1997).

What Makes HAP a Stronger Binding Peptide?

Substitution of three residues in the sequence of the lead peptide resulted in a high affinity peptide (HAP) with an increase of 2 orders of magnitude in its affinity to α -BTX (Kasher et al., 2001). Can our X-ray structure provide explanation for this enhanced affinity? Putting Trp at the N terminus of the peptide (in position 187) adds 2 side chain interactions of the HAP with the toxin, between the indole NE atom and the carbonyl oxygens of residues 6 and 7 of α -BTX (Table 5). Indeed, residue 187 is a Trp in the $\alpha 1$ subunit of TcAChR.

The substitution of Ser196Pro adds to the stability of the binding conformation of the peptide. Proline at this position is found in AChR sequences (196 in the $\alpha 7$ and the homologous 197 in $\alpha 1$). The proline fits well in a hydrophobic pocket. It is situated at the core of the HAP's intramolecular β sheet, and makes stacking interactions with Tyr189 and edge-on interactions with Trp187. The X-ray structure does not explain the benefit of the Lys195Leu substitution. A peptide with Lys in position 195 showed also a tighter binding to α -BTX (Table 1).

Some Surprises Provided by the 1.8 Å Structure

Ten residues in the refined structure show alternate conformations. These are Ser12, Ala31, Cys48, Ser50, Glu56, and Cys59 in α -BTX of monomer A and Ser34, Glu56, and Gln71 in monomer B. Since the two monomers and two HAPs in the asymmetric unit were refined independently (i.e., no noncrystallographic symmetry applied; Table 3), the fact that different residues show alternate conformations in the two monomers reflects the different environments in which these residues are

Table 4. Short Intramolecular Distances (<3.3 Å) in HAP

HAP Residue	Atom	HAP Residue	Atom	Distance (Å) ^a
Arg188	N	Asp199	OXT	3.26 (-)
Arg188	N	Tyr197	O	2.84 (6.37)
Arg188	O	Tyr197	N	2.71 (2.88)
Tyr190	O	Ser193	N	3.21 (3.29)
Tyr190	O	Ser192	N	3.00 (3.19)
Ser193	OG	Leu195	N	2.94 (2.96)
Ser193	OG	Leu194	N	2.94 (2.67)
Pro198	O	Asp199	OXT	3.00 (-)

^a Numbers in parenthesis represent distances in independently refined HAP B.

Table 5. Short Intermolecular Distances between HAP and α -BTX

HAP Residue	Atom	α -BTX Residue	Atom	Distance (\AA) ^a
Trp187	NE1	Thr6	O	3.35 (4.96)
Trp187	NE1	Ala7	O	3.80 (3.45)
Trp187	N	Thr6	O	6.81 (2.90)
Arg188	NH1	Asp30	OD2	3.13 (3.37)
Tyr189	OH	Thr8	O	2.70 (2.59)
Tyr189	OH	Ile11	N	3.35 (3.43)
Tyr189	O	Val40	N	2.86 (2.77)
Tyr190	OH	Asp30	OD2	2.49 (2.55)
Tyr190	O	His68	NE2	2.89 (2.82)
Glu191	OE1	Lys38	N	2.73 (2.70)
Glu191	N	Lys38	O	2.92 (2.91)
Ser192	OG	Arg36	O	2.72 (2.67)
Ser192	N	Arg36	O	3.32 (3.22)
Ser193	O	His68	NE2	3.15 (3.09)
Leu194	CD2	Gln71	NE2	3.02 (3.26)
Tyr197	CZ	Arg36	CD	3.89 (3.79)

^aNumbers in parenthesis represent distances from independently refined monomer B.

located in the crystal. Some of these alternate conformations are of particular interest.

The S-S bond formed by residues Cys48 and Cys59 shows alternate conformations with SG having a dihedral angle χ ca. 120° between two conformations. Each of these bonds is populated by ca. 50% of the residues. This alternate S-S bond is seen only in one of the two independently refined monomers (monomer A).

In the NMR structure determination of α -BTX complexed with TcAChR peptide 185–196 (Basus et al., 1993), residue Ala31 was reported to be Val in some of the α -BTX population. HPLC analysis of the α -BTX

(Sigma cat. No. T3019) has shown the presence of the two species of α -BTX and enabled their separation. The two species do not show any difference in binding to TcAChR (M. Balass, personal communication), or in their tendency to crystallize. Indeed, the X-ray structure shows residue Ala31 to be pointing into the solution, away from the HAP binding surfaces. The structure of monomer A shows alternate α -BTX molecules with ca. 30% having Val31 in the Ala31 position.

The crystal which underwent a quick dip in a 0.3 M KI containing solution before data collection yielded data to much higher resolution (1.8 \AA) compared to the

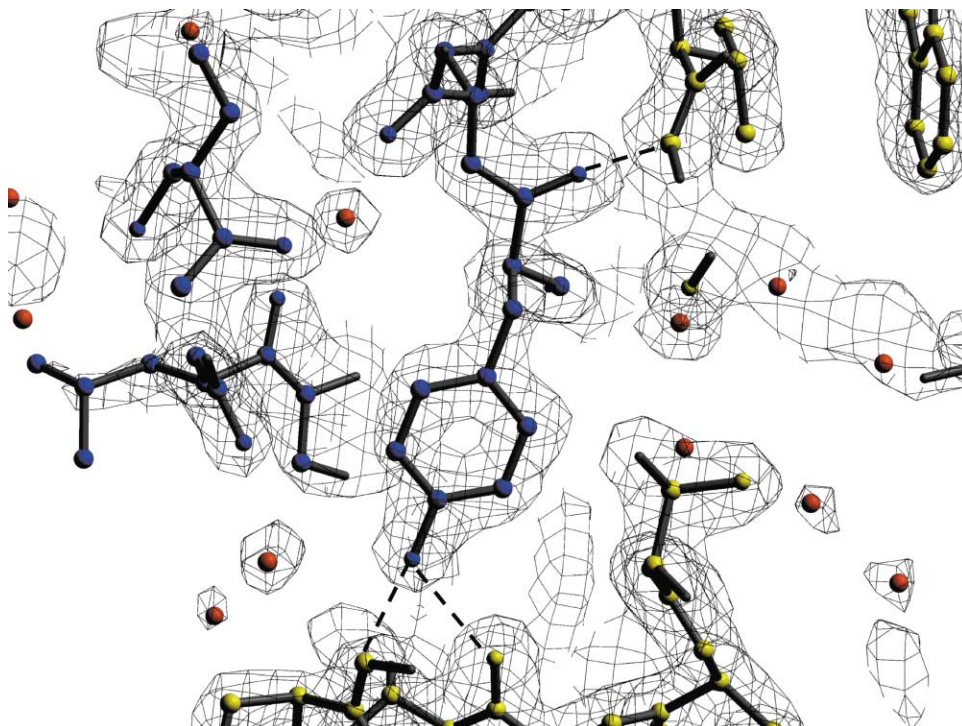


Figure 4. The Snug Fit of Tyr189 of the HAP (Cyan) into a Loop Region of α -BTX (Yellow) Short interactions shown as dashed lines. Water molecules shown in magenta. The composite omit map (Brünger et al., 1998) is drawn at 1.7σ .

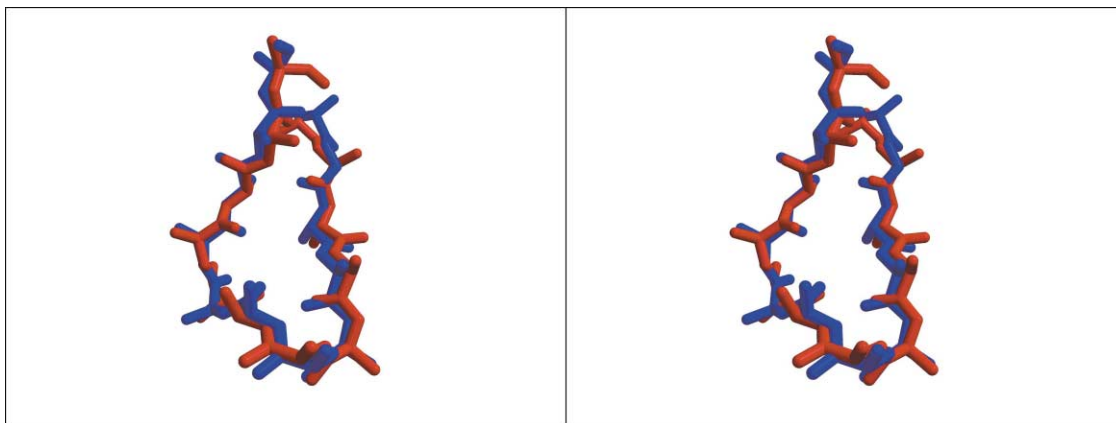


Figure 5. Comparison, in Stereo, of the 3D Structures of HAP (Red) and Loop 182-193 of AChBP (Blue). Only main chain and C^β atoms are shown for clarity.

nonsoaked crystal (2.4 Å), yet the position of the iodine atom could not be located by difference Fourier methods (see Experimental Procedures section). When the structure was refined, two solvent molecules were found to have high residual $F_o - F_c$ density, and their temperature factors refined to the minimum value allowed by the program. Subsequently, these two molecules were refined as partially occupied (40%) iodine ions, resulting in no residual difference density and average temperature factors. Both iodine atoms are located in a pocket formed by Arg25, Met27, Glu56, and Thr58 of monomers A and B. The partial occupancy of the iodine atoms explains the difficulty in locating them in a difference Fourier map and hence the preclusion of their use for providing phasing information as heavy atom deriva-

tives. It is possible that a slightly longer soak (3 min soak was tried) could yield an effective derivative, and this method (Dauter et al., 2000) looks very promising either as a quick way to obtain heavy atom derivatives or better diffracting crystals.

The Binding of α -BTX to AChR

Recently, the structure of acetylcholine binding protein (AChBP) has been determined at 2.7 Å resolution (Brejč et al., 2001). The AChBP modulates synaptic transmission and its sequence is 28.2% identical to that of the extracellular domain of AChR $\alpha 7$ subunit. AChBP binds acetylcholine and antagonists like α -BTX (Smit et al., 2001). The AChBP crystal structure shows it to be a pentamer like the AChR molecule. The ACh binding site

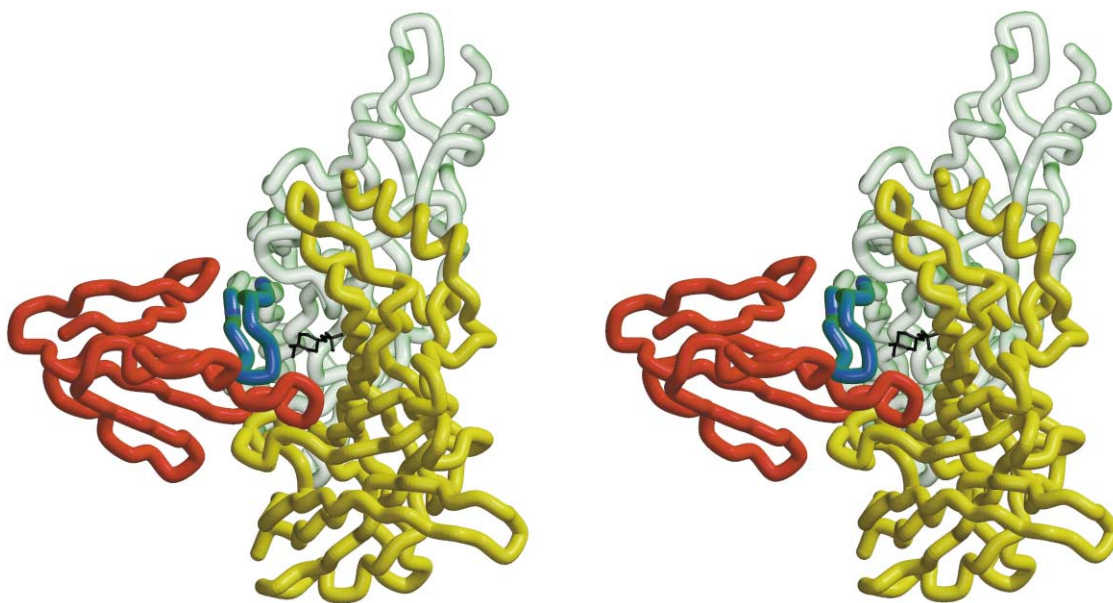


Figure 6. A Stereo View of the Combined Model of α -BTX-HAP (Red) and AChBP Structure with Subunit A in Green and Subunit B in Yellow Showing the Insertion of Loop 2 of the Toxin into the Interface of the Two Subunits

The positively charged HEPES molecule (black stick figure) shows the location of the acetylcholine binding site and the blockage of passage to this site caused by the binding of the toxin. The HAP, which overlaps the 182-193 loop of AChBP, is shown in blue.

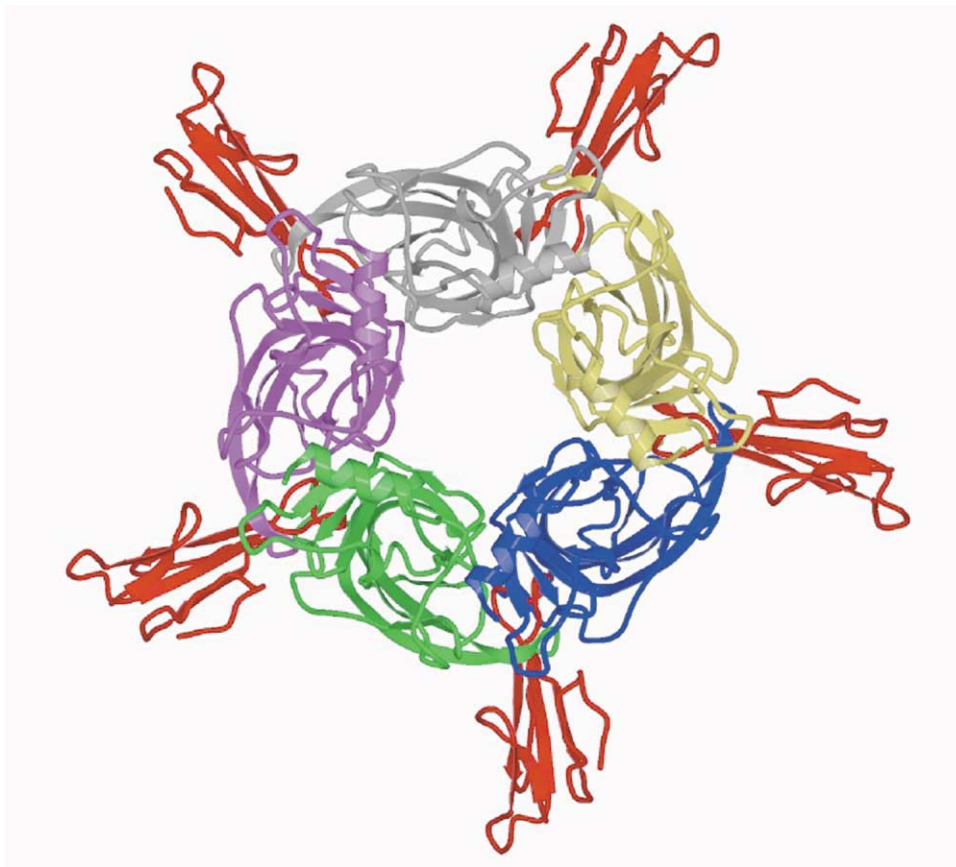


Figure 7. The Combined Model of the AChBP Pentamer with Five Copies of α -BTX (Red) Bound to It, as Viewed down the 5-Fold Axis of the Pentamer

in AChBP was assigned by the localization of a solvent molecule (positively charged HEPES) seen near residues corresponding to the 187–199 loop of the AChR α subunit and stacking on the corresponding Trp143. The AChBP structure is obviously an ideal candidate for testing the relevance of the conformation of the HAP when bound to α -BTX, to that of the corresponding binding region in AChR. The overlay of the first 12 residues of the 13-mer HAP on AChBP residues 182–193 shows the HAP to assume exactly the same conformation as the AChBP loop, and hence probably that of the α -BTX (ACh) binding loop in AChR (Figure 5). Although the sequence of HAP has only three identical residues to the 182–194 loop of AChBP (Table 1), the RMS of C α for the 12 residues is just 0.76 Å. It thus seems that even the short 13-mer binding HAP assumes a structure similar to the corresponding region of AChR upon binding to α -BTX.

The superposition of the HAP on loop 182–193 of AChBP reveals the α -BTX to fit exquisitely into the interface of two subunits of the pentameric AChBP (Figures 6 and 7). Hence, not only does the 182–193 stretch of the AChBP subunit make contacts with fingers 1, 2, and 4 of α -BTX as is seen in the α -BTX-HAP complex (Figures 2 and 3), but in addition, loop 2 of the toxin is inserted into the interface of two adjacent subunits of AChBP with relatively minor clashes between AChBP and α -BTX. It is noteworthy that although the model is

not perfect, there are, in fact, no interactions shorter than 3 Å between main chain atoms of α -BTX and those of the two AChBP subunits with which it interacts. Early crosslinking studies (Karlin et al., 1979; Oswald and Changeux, 1982) have already indicated that α -BTX crosslinks not only to the α subunit, but also to the γ and δ subunit, and support the notion that it binds to $\alpha\gamma$ and $\alpha\delta$ interfaces. Upon binding of α -BTX to the AChBP pentamer in the superposition model, 18% (760 Å²) of the toxin surface becomes inaccessible. It is noteworthy that in this superposition, α -BTX binds perpendicular to the 5-fold axis of the AChBP molecule, and therefore, there are no steric hindrance limitations even when five toxin molecules bind to AChBP (Figure 7).

As is evident from the X-ray structure, the major interactions between α -BTX and the HAP, and by the analogy to the AChR α subunit, occur in residues 187–192 of that subunit. These interactions are listed in Table 5 and shown in Figure 4. The interactions agree with several studies aimed at locating the α -BTX binding domain on the α subunit of AChR (Aronheim et al., 1988; Conti-Tronconi et al., 1990; Neumann et al., 1986b; Ralston et al., 1987; Wilson et al., 1985, 1988; Wilson and Lentz, 1988). Mutational studies of the long chain α -cobratoxin have identified residues 28, 30, 32, 36, 39, and 68 (α -BTX numbering) as involved with binding of the toxin to both neuronal and muscle AChR (Antil-Delbeke et al., 2000).

In our X-ray derived model, these residues are all near the AChBP with nearest C α -C α distance of 5.2, 5.4, 4.4, 6.2, 4.9, and 6.4 Å, respectively.

The superimposed model of AChBP and α -BTX shows residues 34–36 (corresponding to residues 36–38 of AChR δ subunit) and 162–165 (δ 181–184) of the neighboring AChBP subunit (subunit B) as abutting the α -BTX molecule. Selective point mutations of the γ and δ AChR subunits, followed by agonists' binding studies to the resulting AChR mutants, were previously used in order to identify and localize the agonists' binding sites on these subunits. Such studies have identified δ Asp180 or the aligned γ Asp174 (Martin et al., 1996), as well as δ Ser36 or γ Lys34 and δ Ile178 or γ Phe172 (Prince and Sine, 1996), as part of the ACh binding site in AChR, in addition to the major binding loop in the α subunit. All these residues are at, or in very close proximity to, the site in the B subunit of AChBP that interacts with α -BTX. Moreover, this is in agreement with recent studies showing that loop 2 of α -neurotoxins interacts with amino acid residues from the γ , δ , and ϵ subunits, located at the interface of the α subunit (Malany et al., 2000; Osaka et al., 1999, 2000; Sine, 1997). This adds additional weight to the similarity in the ligand binding manner, and 3D structure, of the AChBP pentamer to that of the AChR pentamer.

It is noteworthy that residue Lys38 of α -BTX is near Asp161 of AChBP subunit B, i.e., the homologous AChR δ Asp180 or γ Asp174 identified as part of the ACh binding site (Martin et al., 1996). The possible formation of an intermolecular salt bridge between AChR and α -BTX at that position may provide further explanation to the high affinity of binding of the toxin to the receptor. This notion is supported by recent studies on charge reversal mutations of basic residues on loop 2 of α -neurotoxin (Osaka et al., 2000). These studies indicate electrostatic interactions between the toxin and the γ , δ , and ϵ subunits of AChR. The superimposed model of AChBP and α -BTX suggests that the putative agonist HEPES seen in the AChBP structure is blocked from entering or leaving the AChBP interface cleft by the insertion of loop 2 of α -BTX into that cleft (Figure 6). This clarifies and explains the strong inhibition of AChR function by the toxin.

Experimental Procedures

Synthesis of the HAP

All protected amino acids and coupling reagents were purchased from Novabiochem (Laufelfingen, Switzerland). Solvents for peptide synthesis were of synthesis-grade (Labscan; Dublin, Ireland). HAP was prepared by conventional solid-phase peptide synthesis, using a few reaction vessels of an ABIMED AMS-422 automated solid-phase multiple peptide synthesizer (Langenfeld, Germany). The 9-fluorenylmethoxycarbonyl (Fmoc) strategy was used throughout the peptide chain assembly (Atherton and Sheppard, 1989), following the company's commercial protocols. Wang resin, which contains 25 μ mol of a covalently bound *N*-Fmoc aspartic acid (the first C-terminal residue), was used in each reaction vessel (polymer loading of 0.55 mmol/g). Side chain protecting groups were *tert*-butyloxycarbonyl (*t*-Boc) for Lys; *tert*-butyl-ester (*O*-*t*-But) for Asp and Glu; *tert*-butyl ether (*t*-But) for Ser and Tyr; and pentamethylidihydrobenzofuran-5-sulfonyl (Pbf) for Arg. Coupling was carried out by using two successive reactions with 100 μ mol (4 equiv.) of the corresponding *N*-Fmoc amino acid, 100 μ mol (4 equiv.) of benzotriazole-1-yl-oxy-tris-pyrolidino-phosphonium hexafluorophosphate (PyBop) reagent, and 200 μ mol (8 equiv.) of 4-methyl-morpholine, all

dissolved in dimethylformamide for 20–45 min at room temperature. Cleavage of the peptide from the polymer was performed by reacting the resin of each reaction vessel with 1.8 ml trifluoro-acetic acid (TFA)/H₂O/thioanisole/ethane-dithiol/phenol at volume ratios of 87.5/5/5/2.5/trace amount, for 2 hr at room temperature. The cleavage mixtures were cooled to 4°C; the peptides were precipitated with ice-cold di-*tert*-butylether and centrifuged for 10–15 min, 3000 rpm at 4°C. The pellet was washed and centrifuged three times with di-*tert*-butylether, dissolved in water, and lyophilized. The HPLC-purified HAP was analyzed by time-of-flight mass spectrometry using a VG MALDI TOF mass spectrometer (VG Fisons, Altrincham, UK), and was found to exhibit 1689.7 mass units (calculated 1688.9).

HAP Purification and Analysis by Reversed-Phase HPLC

The synthetic HAP was purified by using a prepacked LiChroCart RP-18 column (10 \times 250 mm, 7 μ m bead size; Merck, Darmstadt, Germany) employing a binary gradient formed from 0.1% TFA in water (solution A) and 0.1% TFA in 75% acetonitrile in water (solution B). The chromatographic run (flow rate 5.0 ml/min) started with 20% solution B in solution A, kept constant for 15 min, followed by a gradient increase of solution B from 20% to 60% over an additional 35 min. The peak was eluted at 37 min. Peptide purification was performed using a Spectra-Physics SP8800 liquid chromatography system equipped with SP8500 dynamic mixer and an Applied Biosystems 757 variable wavelength absorbance detector. The chromatograms were recorded on a Chrom-Jet integrator.

Purity validation of the synthetic HAP was performed by analytical reversed-phase HPLC, using a pre-packed Lichrospher-100 RP-18 column (4 \times 250 mm, 5 μ m bead size; Merck, Darmstadt, Germany) and the same buffer system as described above, except that the gradient started with 5% solution B (flow rate 0.8 ml/min), kept constant for 5 min, and then increased solution B from 5% to 95% over 40 min. The purified HAP eluted at 27.5 min and was >99% pure. The chromatographic analysis was performed using a Spectra-Physics P200 liquid chromatography system equipped with a Spectra-Physics UV100 variable wavelength absorbance detector and AS100 auto sampler. The chromatograms were recorded on a PE Nelson integrator model 1022. All column effluents were monitored by UV absorbance at 220 nm; solvents were obtained from Merck (Darmstadt, Germany).

Preparation of α -BTX-HAP Complex

A solution of the purified HAP (10 mg/ml water, adjusted to pH 7 with 0.5 N NaOH and 0.2 N HCl) was mixed with a solution of α -BTX from the snake venom of *Bungarus multicinctus* (Sigma, product number T3019; 10 mg/ml water) at a volume ratio of 1:3.3, respectively, to give a molar ratio of 1.5:1 HAP: α -BTX. The resulting solution (measured pH 7) was incubated overnight at 4°C for complex formation, centrifuged (5 min, 14000 rpm), and was used for crystallization. α -BTX-HAP crystals were grown by the hanging drop method at 19°C from a solution containing 10 mg/ml of the complex. This solution was diluted at the ratio of 3:1 with the reservoir solution, whose composition was 40% polyethylene glycol 3350, 0.1 M PIPES buffer pH 7.5. Crystals grew in 3 days as rectangular prisms, 0.3 \times 0.1 \times 0.1 mm in size, space group C222₁.

Data collection, Structure Determination, and Refinement

X-ray data to 2.4 Å resolution (Table 2) were collected on an R-AXIS-II detector at 100 K, from a single crystal that had been dipped in oil. Attempts at solving the crystal structure by molecular replacement (AMoRe program (Navaza, 1994)) using as starting model either the X-ray structure of α -BTX (Protein Data Bank code 2abx; Love and Stroud, 1986) or the NMR structure of α -BTX-lead peptide complex (Protein Data Bank code 2btx; Scherf et al., 1997) produced very low peaks with poor correlation, and all the solutions showed severe clashes with symmetry-related molecules. In an effort to get a suitable heavy atom derivative, we used the method developed by Dauter which uses quick soaking of a crystal in mother liquor containing halides such as Br or I (Dauter et al., 2000). An α -BTX-HAP crystal was soaked in mother liquor solution containing 0.3 M KI for 3 min, then transferred to oil and flash cooled. This crystal diffracted to a much higher resolution, i.e., 1.8 Å (Table 2), but the iodine binding sites could not be located using anomalous Patterson or

difference Fourier methods (Results and Discussion section). As with the first data set, this higher resolution data set did not yield a molecular replacement solution. At this stage, we reconsidered the X-ray structure starting model which was being used for molecular replacement, as this structure, Protein Data Bank ID code 2abx (Love and Stroud, 1986), has a number of outliers in its Ramachandran plot, and appears to be built of nonstandard 3D structural building blocks (Unger et al., 1989). A FASTA (Pearson, 1990) search of sequences similar to α -BTX in the Protein Data Bank database identified two structures as having the highest homology to α -BTX. These are: neurotoxin-I, Protein Data Bank code 1ntn (Mikhailov et al., 1990) (62.1% identity) and α -cobratoxin, Protein Data Bank code 2ctx (Betz et al., 1991) (55.4% identity). The two toxin structures overlaid reasonably well with the X-ray structure of α -BTX (2abx), but diverged at their C termini. We therefore chose as a search model the first 66 residues of the structure of neurotoxin-I (Protein Data Bank ID code 1ntn) deleting eight residues from the C terminus. Molecular replacement search was run with program MOLREP (Vagin and Teplyakov, 1997), resulting in a clear peak with $R = 53.9\%$ and correlation = 0.277 (the next best peak had values of $R = 57.5\%$, correlation = 0.172), and no clashes were observed between symmetry-related molecules. MOLREP yielded coordinates for two independent monomers in the asymmetric unit.

The structure was refined with CNS (Brünger et al., 1998), using the maximum likelihood, slow cooling option. All measured reflections were used in the refinement, and the two monomers and two HAPs were refined independently, i.e., without the application of noncrystallographic symmetry restraints. The F_{obs} were scaled anisotropically and a bulk solvent correction was applied (Brünger et al., 1998). The structure was fitted into the electron density with the program O (Jones et al., 1991). The missing C-terminal residues as well as an insertion of α -BTX residues 13–14 were clearly visible in the difference electron density. Density for the HAP peptide was seen, but fitting was complicated by its close proximity to the α -BTX density. The warpNtrace option in program ARP_wARP successfully traced nine amino acids of one HAP and ten of the other. 116 of the solvent molecules (out of 217) were found by program wARP_REFMAC (Perrakis et al., 1997, 1999).

Acknowledgments

This work was supported in part by the U.S. Army Medical Research Acquisition Activity under Contract No. DAMD17-97-2-7022 and the Kimmelman Center for Biomolecular Structure and Assembly, Israel to J.L.S., and by the Muscular Dystrophy Association of America (MDA) and the Association Française Contre les Myopathies (AFM) to S.F.

Received June 5, 2001; revised September 4, 2001.

References

Antil-Delbeke, S., Gaillard, C., Tamiya, T., Corringier, P.J.-Y., Changeux, J.-P., Servent, D., and Ménez, A. (2000). Molecular determinants by which a long chain toxin from snake venom interacts with the neuronal $\alpha 7$ -nicotinic acetylcholine receptor. *J. Biol. Chem.* **275**, 29594–29601.

Aronheim, A., Eshel, Y., Mosckovitz, R., and Gershoni, J.M. (1988). Characterization of the binding of alpha-bungarotoxin to bacterially expressed cholinergic binding sites. *J. Biol. Chem.* **263**, 9933–9937.

Atherton, E., and Sheppard, R.C. (1989). *Solid Phase Peptide Synthesis. A Practical Approach* (New York: IRL Oxford University Press).

Balass, M., Katchalski-Katzir, E., and Fuchs, S. (1997). The α -bungarotoxin binding site on the nicotinic acetylcholine receptor: Analysis using a phage-epitope library. *Proc. Natl. Acad. Sci. USA* **94**, 6054–6058.

Barchan, D., Kachalsky, S., Neumann, D., Vogel, Z., Ovadia, M., Kochva, E., and Fuchs, S. (1992). How the mongoose can fight the snake: The binding site of the mongoose acetylcholine receptor. *Proc. Natl. Acad. Sci. USA* **89**, 7717–7721.

Barchan, D., Ovadia, M., Kochva, E., and Fuchs, S. (1995). The

binding site of the nicotinic acetylcholine receptor in animal species resistant to alpha-bungarotoxin. *Biochemistry* **34**, 9172–9176.

Basus, V.J., Song, G., and Hawrot, E. (1993). NMR solution structure of an alpha-bungarotoxin/nicotinic receptor peptide complex. *Biochemistry* **32**, 12290–12298.

Betz et al., C., Lange, G., Pal, G.P., Wilson, K.S., Maelicke, A., and Saenger, W. (1991). The refined crystal structure of alpha-cobratoxin from *Naja naja siamensis* at 2.4-Å resolution. *J. Biol. Chem.* **266**, 21530–21536.

Brejck, K., van Dijk, W.J., Klaassen, R.V., Schuurmans, M., van der Oost, J., Smit, A.B., and Sixma, T.K. (2001). Crystal structure of an ACh-binding protein reveals the ligand-binding domain of nicotinic receptors. *Nature* **411**, 269–276.

Brünger, A.T., Adams, P.D., Clore, G.M., DeLano, W.L., Gros, P., Grosse-Kunstleve, R.W., Jiang, J.S., Kuszewski, J., Nilges, M., Pannu, N.S., et al. (1998). Crystallography & NMR system: A new software suite for macromolecular structure determination. *Acta Cryst. D54*, 905–921.

Changeux, J.-P., and Edelstein, S.J. (1998). Allosteric receptors after 30 years. *Neuron* **21**, 959–980.

Changeux, J.-P., Kasai, M., and Lee, C.Y. (1970). The use of a snake venom toxin to characterize the cholinergic receptor protein. *Proc. Natl. Acad. Sci. USA* **67**, 1241–1247.

Conti-Tronconi, B.M., Tang, F., Diethelm, B.M., Spencer, S.R., Reinhardt-Maelicke, S., and Maelicke, A. (1990). Mapping of a cholinergic binding site by means of synthetic peptides, monoclonal antibodies, and alpha-bungarotoxin. *Biochemistry* **29**, 6221–6230.

Dauter, Z., Dauter, M., and Rajashankar, K.R. (2000). Novel approach to phasing proteins: derivatization by short cryo-soaking with halides. *Acta Cryst. D56*, 232–237.

Jones, T.A., Zou, J.-Y., Cowan, S.W., and Kjeldgaard, M. (1991). Improved methods for building protein models in electron density maps and the location of errors in these models. *Acta Cryst. A47*, 110–119.

Kachalsky, S.G., Jensen, B.S., Barchan, D., and Fuchs, S. (1995). Two subsites in the binding domain of the acetylcholine receptor: An aromatic subsite and a proline subsite. *Proc. Natl. Acad. Sci. USA* **92**, 10801–10805.

Kao, P., Dwork, A., Kaldany, R., Silver, M., Weideman, J., Stein, S., and Karlin, A. (1984). Identification of the α -subunit half-cysteine specifically labeled by an affinity reagent for the acetylcholine receptor binding site. *J. Biol. Chem.* **259**, 11662–11665.

Karlin, A., and Akabas, M.H. (1995). Toward a structural basis for the function of nicotinic acetylcholine receptors and their cousins. *Neuron* **15**, 1231–1244.

Karlin, A., Damle, V., Hamilton, S., McLaughlin, M., Valderamma, R., and Wise, D. (1979). Acetylcholine receptors in and out of membranes. *Adv. Cytopharmacol.* **3**, 183–189.

Kasher, R., Balass, M., Scherf, T., Fridkin, M., Fuchs, S., and Katchalski-Katzir, E. (2001). Design and synthesis of peptides that bind α -bungarotoxin with high affinity. *Synth. Biol.* **8**, 147–155.

Laskowski, R.A., MacArthur, M.W., Moss, D., and Thornton, J.M. (1993). PROCHECK: A program to check the stereochemical quality of protein structures. *J. Appl. Cryst.* **26**, 283–291.

Lee, C.Y., and Chang, C.C. (1966). Modes of actions of purified toxins from elapid venoms on neuromuscular transmission. *Mem. Inst. Butantan* **33**, 555–572.

Lentz, T.L. (1995). Differential binding of nicotine and alpha-bungarotoxin to residues 173–204 of the nicotinic acetylcholine receptor alpha 1 subunit. *Biochemistry* **34**, 1316–1322.

Love, R.A., and Stroud, R.M. (1986). The crystal structure of alpha-bungarotoxin at 2.5 Å resolution: relation to solution structure and binding to acetylcholine receptor. *Protein Eng.* **1**, 37–46.

Malany, S., Osaka, H., Sine, S.M., and Taylor, P. (2000). Orientation of alpha-neurotoxin at the subunit interfaces of the nicotinic acetylcholine receptor. *Biochemistry* **39**, 15388–15398.

Martin, M., Czajkowski, C., and Karlin, A. (1996). The contributions of aspartyl residues in the acetylcholine receptor gamma and delta

- subunits to the binding of agonists and competitive antagonists. *J. Biol. Chem.* **271**, 13497–13503.
- Michalet, S., Teixeira, F., Gilquin, B., Mourier, G., Servent, D., Drevet, P., Binder, P., Tzartos, S., Ménez, A., and Kessler, P. (2000). Relative spatial position of a snake neurotoxin and the reduced disulfide bond α (Cys192–Cys193) at the $\alpha\gamma$ interface of the nicotinic acetylcholine receptor. *J. Biol. Chem.* **275**, 25608–25615.
- Mikhailov, A.M., Nickitenko, A.V., Trakhanov, S.D., Vainshtein, B.K., and Chetverina, E.V. (1990). Crystallization and preliminary x-ray diffraction study of neurotoxin-I from *Naja naja oxiana* venom. *FEBS Lett.* **269**, 255–257.
- MSI. (1998). WebLabViewerLite software (San Diego: Molecular Simulations Inc.).
- Navaza, J. (1994). AMORE - an automated procedure for molecular replacement. *Acta Cryst. D50*, 157–163.
- Neumann, D., Gershoni, G.M., Fridkin, M., and Fuchs, S. (1985). Antibodies to synthetic peptides as probes for the binding site on the α -subunit of the acetylcholine receptor. *Proc. Natl. Acad. Sci. USA* **82**, 3490–3493.
- Neumann, D., Barchan, D., Fridkin, M., and Fuchs, S. (1986a). Analysis of ligand binding to the synthetic dodecapeptide 185–196 of the acetylcholine receptor α -subunit. *Proc. Natl. Acad. Sci. USA* **83**, 9250–9253.
- Neumann, D., Barchan, D., Safran, A., Gershoni, J.M., and Fuchs, S. (1986b). Mapping of the α -bungarotoxin binding site within the α subunit of the acetylcholine receptor. *Proc. Natl. Acad. Sci. USA* **83**, 3008–3011.
- Neumann, D., Barchan, D., Horowitz, M., Kochva, E., and Fuchs, S. (1989). Snake acetylcholine receptor: Cloning of the domain containing the four extracellular cysteines of the α -subunit. *Proc. Natl. Acad. Sci. USA* **86**, 7255–7259.
- Osaka, H., Malany, S., Kanter, J.R., Sine, S.M., and Taylor, P. (1999). Subunit interface selectivity of the alpha-neurotoxins for the nicotinic acetylcholine receptor. *J. Biol. Chem.* **274**, 9581–9586.
- Osaka, H., Malany, S., Molles, B.E., Sine, S.M., and Taylor, P. (2000). Pairwise electrostatic interactions between alpha-neurotoxins and gamma, delta, and epsilon subunits of the nicotinic acetylcholine receptor. *J. Biol. Chem.* **275**, 5478–5484.
- Oswald, R.E., and Changeux, J.-P. (1982). Crosslinking of α -bungarotoxin to the acetylcholine receptor from *Torpedo marmorata* by ultraviolet light irradiation. *FEBS Lett.* **139**, 225–229.
- Pearson, W.R. (1990). Rapid and sensitive sequence comparison with FASTP and FASTA. *Methods Enzymol.* **183**, 63–98.
- Perrakis, A., Sixma, T.K., Wilson, K.S., and Lamzin, V.S. (1997). wARP: improvement and extension of crystallographic phases by weighted averaging of multiple-refined dummy atomic models. *Acta Cryst. D53*, 448–455.
- Perrakis, A., Morris, R., and Lamzin, V.S. (1999). Automated protein model building combined with iterative structure refinement. *Nat. Struct. Biol.* **6**, 458–463.
- Prince, R.J., and Sine, S.M. (1996). Molecular dissection of subunit interfaces in the acetylcholine receptor. Identification of residues that determine agonist selectivity. *J. Biol. Chem.* **271**, 25770–25777.
- Ralston, S., Sarin, V., Thanh, H.L., Rivier, J., Fox, J.L., and Lindstrom, J. (1987). Synthetic peptides used to locate the alpha-bungarotoxin binding site and immunogenic regions on alpha subunits of the nicotinic acetylcholine receptor. *Biochemistry* **26**, 3261–3266.
- Samson, A.O., Chill, J.H., Rodriguez, E., Scherf, T., and Anglister, J. (2001). NMR mapping and secondary structure determination of the major acetylcholine receptor α -subunit determinant interacting with α -bungarotoxin. *Biochemistry* **40**, 5464–5473.
- Scherf, T., Balass, M., Fuchs, S., Katchalski-Katzir, E., and Anglister, J. (1997). Three-dimensional solution structure of the complex of α -bungarotoxin with a library-derived peptide. *Proc. Natl. Acad. Sci. USA* **94**, 6059–6064.
- Scherf, T., Kasher, R., Balass, M., Fridkin, M., Fuchs, S., and Katchalski-Katzir, E. (2001). A β -hairpin structure in a 13-mer peptide that binds α -bungarotoxin with high-affinity and neutralizes its toxicity. *Proc. Natl. Acad. Sci. USA* **98**, 6629–6634.
- Sine, S.M. (1997). Identification of equivalent residues in the gamma, delta, and epsilon subunits of the nicotinic receptor that contribute to alpha-bungarotoxin binding. *J. Biol. Chem.* **272**, 23521–23527.
- Smit, A.B., Syed, N.I., Schaap, D., van Minnen, J., Klumperman, J., Kits, K.S., Lodder, H., van der Schors, R.C., van Elk, R., Sorgedrager, B., et al. (2001). A glia-derived acetylcholine-binding protein that modulates synaptic transmission. *Nature* **411**, 261–268.
- Tzartos, S.J., and Changeux, J.P. (1984). Lipid-dependent recovery of alpha-bungarotoxin and monoclonal antibody binding to the purified alpha-subunit from *Torpedo marmorata* acetylcholine receptor. Enhancement by noncompetitive channel blockers. *J. Biol. Chem.* **259**, 11512–11519.
- Unger, R., Harel, D., Wherland, S., and Sussman, J.L. (1989). A 3D building blocks approach to analyzing and predicting structure of proteins. *Proteins Struct. Funct. Genet.* **5**, 355–373.
- Vagin, A., and Teplyakov, A. (1997). MOLREP: an automated program for molecular replacement. *J. Appl. Cryst.* **30**, 1022–1025.
- Wilson, P.T., and Lentz, T.L. (1988). Binding of alpha-bungarotoxin to synthetic peptides corresponding to residues 173–204 of the alpha subunit of *Torpedo*, calf, and human acetylcholine receptor and restoration of high-affinity binding by sodium dodecyl sulfate. *Biochemistry* **27**, 6667–6674.
- Wilson, P.T., Lentz, T.L., and Hawrot, E. (1985). Determination of the primary amino acid sequence specifying the alpha-bungarotoxin binding site on the alpha subunit of the acetylcholine receptor from *Torpedo californica*. *Proc. Natl. Acad. Sci. USA* **82**, 8790–8794.
- Wilson, P.T., Hawrot, E., and Lentz, T.L. (1988). Distribution of alpha-bungarotoxin binding sites over residues 173–204 of the alpha subunit of the acetylcholine receptor. *Mol. Pharmacol.* **34**, 643–650.
- Zeng, H., Moise, L., Grant, M.A., and Hawrot, E. (2001). The solution structure of the complex formed between alpha-bungarotoxin and an 18mer cognate peptide derived from the alpha1 subunit of the nicotinic acetylcholine receptor from *torpedo californica*. *J. Biol. Chem.* **276**, 22930–22940.

Accession Numbers

The atomic coordinates and structure factors for α -BTX-HAP have been deposited at the Protein Data Bank with ID code 1hc9.